Middle-East Journal of Scientific Research 22 (7): 1044-1051, 2014
ISSN 1990-9233

DOI: 10.5829/idosi.mejsr.2014.22.07.21961

Reverse Water Gas Shift Reaction over Tungsten Carbide Prepared Catalyst from Waste Date Palm Fronds at Low Temperature Reverse Water Gas Shift Reaction

Salma Mohamed Saleh Omar and Issa Mohamed Saleh Omar

Department of Chemistry, Faculty of Science, Benghazi University, Benghazi, Libya

Abstract: The reverse water gas shift reaction over prepared tungsten carbide alloy (WC\AC) from date palm fronds catalyst was studied by CO_2 hydrogenation, temperature-programmed reduction of the WC\AC catalyst. In comparison with the reaction of CO_2 alone, hydrogen can significantly promote the CO formation in the RWGS reaction. The formate derived from association of H_2 and CO_2 is proposed to be the key intermediate for CO production. Formate dissociation mechanism is the major reaction route for CO production. The reverse water gas shift (RWGS) reaction over WC/AC with potassium (K) promoter was studied by means of CO_2 hydrogenation at temperature programmed. The main role of Potassium oxide (K_2O) was to provide catalytic activity for decomposition of formats, besides acting as a promoter for CO_2 adsorption. Hydrogen was dissociatively adsorbed on WC/AC and could spill over to K_2O to associate with CO_2. This resulted in the formation of formate species for the production of CO. The activation energy is determined as -27.94 kJ/mol for RWGS synthesis on WC/AC-K from $CO_2 + H_2$.

Key words: Activated carbon · Date palm frond · Microwave · Potassium hydroxide · Tungsten Carbide · Reverse water gas shift · WC\AC catalysts

INTRODUCTION

The initiative of green chemistry arises from the need for sustainable development, where activities embarked on by chemists are basically centered on large-scale processes, products and services that balance advancements in quality of life with the preservation of human health and the environment [1]. For instance, activated carbon (AC) has been applied for industrial wastewater treatment and as a catalyst or catalyst support because of its characteristic adsorption properties [2]. Waste materials are regarded as the most suitable source materials for the production of activated carbon because of their low purchasing cost and easy accessibility [3]. Thus, generating activated carbons from a range of raw materials such as, agricultural wastes, coconut shells and wood will reduce the environmental impact of waste materials. With their use as activated carbon, a high added value can be obtained [4].

In the present study, the activated carbons were prepared from waste date palm fronds (DPF). DPF was selected as activated carbon precursors because of their availability and only little work has been done on this material. To the best of our knowledge, influence of activating agents on the adsorption capacity of activated carbons made from DPF has not been well investigated. The aim of the present work is to study the effects of activating agents on the adsorption capacity of the activated carbon prepared from date palm fronds. Several chemical activating agents have been used in the preparation of activated carbon. Potassium hydroxide is the widely preferred chemical activating agent. In this paper, we will study the effect of potassium in improving the performance of the use of carbon made from raw materials in the production of tungsten carbide. The effectiveness of carbide catalyst has been analyzed in studies of Levy and Boudart, where they studied tungsten carbide as a potential alternative to precious metal catalysts. Other catalysts that have also been extensively studied include molybdenum and tungsten carbide. The catalytic behavior of the carbides is determined by their surface chemistry [5].

Currently, microwave power also plays a crucial part in adsorption capacity and carbon yield and microwave induced alloying. Increasing microwave power from 90 to 600W considerably enhances yield, possibly because of the combined effect of internal and volumetric heating [6].

Corresponding Author: Salma Mohamed Saleh Omar, Department of Chemistry, Faculty of Science, Benghazi University, Benghazi, Libya. E-mail: salma84m@yahoo.com.

This study aimed to prepare chemical activated carbons from date palm fronds waste and using KOH as the activating agent. The best and optimized carbon was then selected for tungsten carbide microwave induce synthesis reactions. The main objective for this study is to synthesize tungsten carbide using microwave induced from the prepared carbon and tungsten hexacarbonyl {$W(CO)_6$} as the precursor. The K moiety present in the carbon is expected to enhance both the induce microwave alloying.

The reverse water gas shift (RWGS) reaction had known to chemistry since the mid 1800's [7]. RWGS reaction was one of the fundamental reactions which occur during supercritical water gasification [8]. RWGS reaction is an equilibrium reaction and the conversion of CO_2 to CO is depending on temperature. Although high temperature reactions are effective for obtaining a high conversion, studies on the reactions at temperatures above 873K are limited. The conversion of carbon dioxide to carbon monoxide by catalytic hydrogenation had recognized as a very promising process. In industry, synthesis gas containing hydrogen and carbon monoxide can be used to prepare CH_3OH as well as long chain hydrocarbons via the Fischer-Tropsch synthesis. Therefore, the reverse water gas shift (RWGS) reaction (as shown equation 1.1) was an important option for carbon monoxide production [9] and [10].

$$CO_2 + H_2 \leftrightarrow CO + H_2O. \quad (1.1)$$

The Water Gas Shift Reaction (WGSR) is an important industrial reaction for the production of chemicals or H_2, was expected to play a key role in the integration of gasification technologies with a hydrogen production/recovery unit. The effluent stream of the gasifier, mainly hydrogen, carbon monoxide and carbon dioxide at high pressure reach to 30 atm and temperatures reach to 400-1000°C, would be directed to the water gas shift reactor along with steam where reaction (Eq 1.2) will take place, increasing the yield of hydrogen [11] and [12].

$$CO_2 + H_2 \leftrightarrow CO + H_2O \ \Delta H = -40.6 \text{ KJ/mol}. \quad (1.2)$$

The RWGS reaction was an exothermic, equilibrium-limited reaction that exhibits decreasing conversion with increasing temperature. Reviews of the catalyzed WGSR were at temperatures below 600°C. A catalyst is required under these conditions because of the lower reaction rate at low temperature. There has been renewed interest in the RWGS reaction at extreme temperatures however, because of recent advances in high-temperature materials for hydrogen separation membranes. The permeation of hydrogen through the walls of a membrane reactor enables the attainment of high conversion of carbon monoxide and steam to H_2 and CO_2 [13].

According to Tingey *et al*, 1966 [14] studied the RWGS reaction over an extended temperature range (400-1200°C) and indicate to that at high-temperature (>800°C), the reaction would follow the chain reaction mechanism but would follow a different mechanism at lower temperature [7]. All of these studies are performed in highly diluted reaction gas mixture at ambient pressure, without exploring the influence of pressure on the reaction rate and kinetics. The utility of the high-temperature, non-catalytic RWGS reaction is supported by these previous results showing high reaction rates at extreme temperatures This report will address the kinetics of the reverse water gas shift reaction under conditions not studied previously, namely high concentration streams, non-diluted streams and high-pressures. These conditions are more suitable to draw conclusions on the application of the water gas shift reaction directly to a gasification stream by membrane reactor [13].

Based on adopted catalysts or reaction temperature, RWGS was generally classified into two different reactions; one is the high-temperature shift reaction (HTSR) and the other the low temperature shift reaction (LTSR). HTSR is approximately operated at the temperatures between 350 and 500 °C and the typical adopted catalysts are Fe-Cr-based catalysts. In contrast, the temperature of LTSR is usually in the range of 150 to 250°C [15] and Cu-Zn-based catalysts are the most commonly used ones. On the one hand, from Arrhenius law it is known that increasing reaction temperature will facilitate the reaction rate of CO; on the other hand, according to thermodynamics or Le Chatelier's principle a lower reaction temperature is conducive to CO conversion or hydrogen yield, as a consequence of the exothermic reaction involved. In general, HTSR is governed by chemical kinetics, whereas LTSR is dominated by thermodynamic equilibrium.

Experimental: In this section, the material and method that are used in this paper are given as follows.

MATERIAL AND METHODS

Waste date palm frond was used as the precursor for the preparation of activated carbon. The raw material was obtained from Riyadh, Saudi Arabia.

Preparation of Activated Carbon (AC): In this study, the date palm fronds (DPF) were cut into small pieces of about 1-2 cm, washed with water and subsequently dried under the sun. These steps were followed by the crushing and sieving of the particles to mesh size of 1–4 mm. The palm pieces were then washed with hot water and further subjected to heat from the sun to remove any moisture content. Thereafter, the samples were wrapped in aluminum foil and carbonized at 400°C for 2 hours in an evaporating dish at a heating rate of 30°C/min. The resulting char was soaked in potassium hydroxide (KOH) solution with ratio of 1:1, 1:2, 1:3 (w/w%) respectively for 24 hours. The sample was then activated at power 360-630W. The activated product was then cooled to room temperature and washed with 0.1 M hydrochloric acid and afterward with hot distilled water.

Preparation of Tungsten Carbide: In this study, the prepared carbon would be used in microwave induce alloying to prepared tungsten carbide. The effect of KOH concentration uses also the observed in preparing the catalyst, tungsten hexacarbonyl powder was mixed with the appropriate amount of the activated carbon.

Catalytic Testing Hydrogenation Reaction of Carbon Dioxide: Prior to the catalytic reaction, the prepared catalyst was reduced in hydrogen gas flow using a tube furnace. The catalyst was heated at 400°C at the rate of 5 °C/min and hold at 400°C for 1 hour. Then about 1 g of the reduced catalyst was placed in the glass micro reactor. The hydrogenation reaction of carbon dioxide (H_2/CO_2) was conducted in a glass flow system at temperature ranging from 100 to 400°C. However, the composition of the product evolved at the reactor outlet was collected in gas collector and were analyzed using Fourier transform infrared spectroscopy (FTIR).

RESULTS AND DISCUSSION

In this section, we provide our main results.

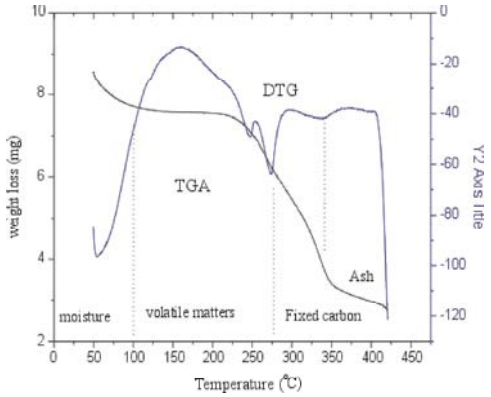

Fig. 3.1: TGA Proximate analysis of date palm frond using thermogravimetry.

Characterization of Activated Carbon and Tungsten Carbide

Themogravimetry Analysis of Raw Date Palm Fronds (Raw-DPF): To study the suitably of date palm frond, TGA characterization was carried. The percentage of weight loss during thermogravimetric analysis for dates palm frond is shown in Figure 3.1 and Table 3.1. The TGA results show total percentages composition of date palm fronds. As seen from the graph, the first range of decomposition occurred at 50-100°C, which represents 13.5% weight lost, possibly as a result of surface moisture released from the sample during heating. The second phase of decomposition ranged from 100-270°C, which indicates further moisture, some bonded water and light hydrocarbon. Further on, weight lost of about 79.8% occurred within a temperature range of 270-300°C. This is most probably represented by chemical bonded water and the break down or the decomposition of cellulose, hemicellulose and lignin to carbon. Advance heating above 350°C results in weight loss of about 2.2%, which indicates the elimination of volatile materials formed from the activated carbon produced, such as CO and CO_2. Thus, continual heating will only decrease the amount of products the high surface area carbon generated [16], [17] and [18].

Table 3.1: Proximate analysis of the different materials

		Proximate analysis			
Ref	Sample	Moisture	Volatile matter	Fixed carbon	Ash
Sukiran (2008).	Oil palm shell	5.73%	73.74%	18.37%	2.21%
Azali *et al*. (2005).	Oil palm fiber	6.56%	75.99%	12.39%	5.33%
Trangkaprasith and Chavalparit (2010).	Oil palm frond	7.39%	72.53%	5.81%	14.27%
This study	Date palm fronds	13.5%	79.8%	4.5%	2.2%

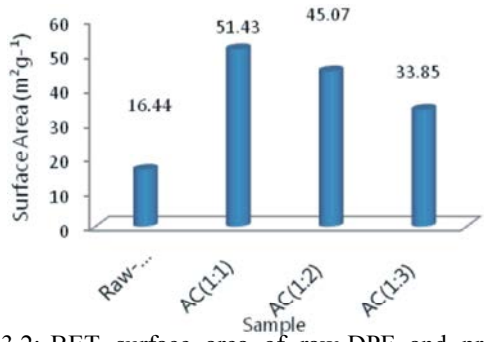

Fig. 3.2: BET surface area of raw-DPF and prepared activated carbons

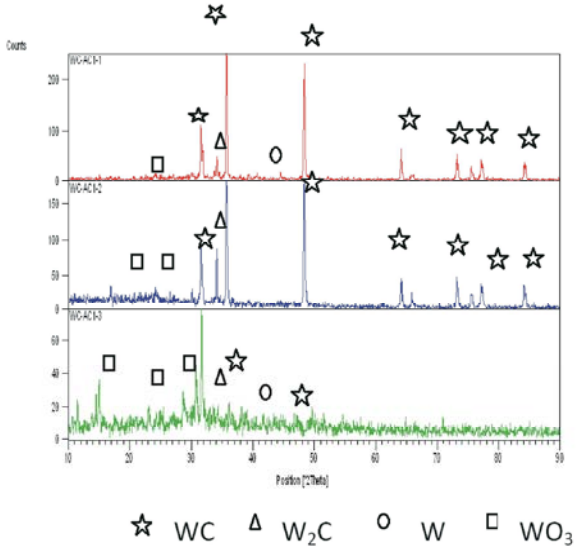

Fig. 3.3: X-ray diffractogram of samples with WC prepared from $\{W(CO)_6\}$ content supported on AC_s

Proximate Analysis: The proximate analysis tells us about the moisture content of the fuel, the amount of volatile components, the fixed carbon and the ash content. The data are usually presented on dry basis. Currently, there are several methods available in the literature that can be used to calculate proximate analysis parameters [19] and [20].

N_2 Adsorption Analysis of Raw-DPF and Prepared Activated Carbon: The N_2 adsorption analysis was carried to study the effect of the chemical activating agent (KOH) on the surface area of the prepared carbon samples. All the data collected, including the Raw-DPF, AC(1:1), AC(1:2) and AC(1:3) respectively are plotted in Figure 3.2. The raw-DPF gives a BET surface area of 16.44 m^2g^{-1} while that for AC(1:1) is 51.43 m^2g^{-1}, followed by AC(1:2) and AC(1:3), which gave values of 45.07 and 33.85 respectively. This result suggests that KOH slightly contributed to modify the surface area of activated carbon. Activated carbon responded to the method involving activation.

The effect of oxidation on BET surface areas varies according to the treatment used and the raw material properties [21-24]. Pore volume and pore size development are in general affected by oxygen chemisorption on pore walls (volume reduction) and oxidation of the carbon material (widening and/or formation of new pores) [25]. According to the results of this work, oxygen chemisorption prevailed over carbon oxidation resulting to a decrease in surface area and pore volumes. Nevertheless, at low temperatures and extended reaction times chemisorption was favored producing modified activated carbons with a high percentage of oxygen functionalities and a slightly modified pore structure.

XRD Analysis on Tungsten Carbide Catalyst Supported on AC-KOH: In this study, the effect of KOH activation ratio focus microwave induced alloy was recorded using XRD. Scanning 2θ from 10° to 90°, the WC film exhibits the following characteristic features: 2θ=30°, WC111; 2θ= 31.6°, WC 001; 2θ = 35.8°, WC100; 2θ = 48.4°, WC 101; 2θ = 64.8°-65.2°, WC 101; 2θ = 73.4° WC111 and 2θ =76.5-76.8° WC102. X-ray powder diffraction analysis of the WC/AC_x catalysts prepared on activated carbon and showed the formation of the W2C crystalline phase was characteristic features: 2θ = 34.2° and 34.5°, W_2C 100; 2θ = 39.8°, W_2C101 during carbonization at 360-630W only on carbon support as in Figure 3.3. However, it is possible, that on other carbon supports the W_2C phase was very well dispersed; the W_2C particles were too small to be detected by XRD. On the other hand, in all samples the characteristic peaks for the metal tungsten (2θ = 40°, W 110) were detected. As shown in Figure 3.3, the peak of (002) planes at 2θ = 24.9°, WO_3 (002).

In this result WC/AC(1:2), there were no significant difference between WC/AC(1:2) and the pattern WC/AC(1:1), as it shows the difference only in the appearance of an extra peak at the 2θ of 17° and 24.5° and corresponding to the (1 1 1) and (2 2 0) facets of WO_3, the 2θ of 30.4°, 31.6°, 35.7°, 48.4°, 64.1°-65.9°, 73.3°, 75.9°, 77.2° and 84.3° and corresponding to the (0 1 1), (0 0 1), (1 0 0), (1 0 1), (1 0 1), (1 1 1) (2 0 1), (1 0 2) and (2 0 1) faces of WC. At 2θ of 34.3° are corresponding to the (1 0 0) face of W_2C.

As shown in Figure 3.3 gives the XRD patterns of the WC/AC(1:3) unlike pattern of WC/AC(1:1) and WC/AC(1:2). There are some similar peaks of WC/AC(1:1)

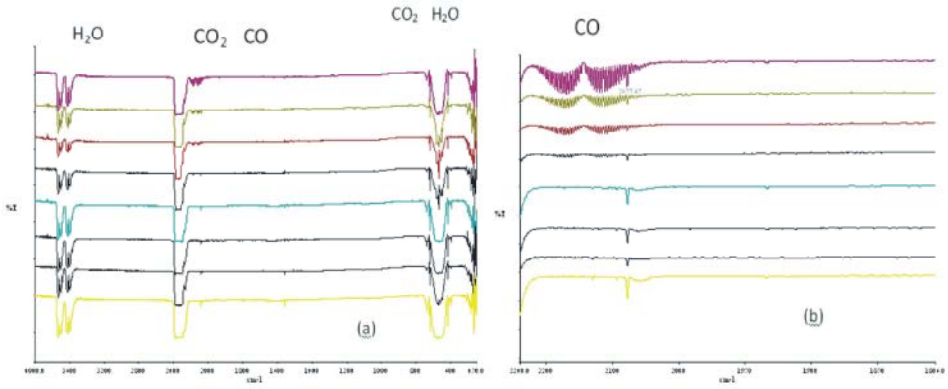

Fig. 3.4: FTIR spectra of (a) = CO2 hydrogenation over catalyst WC/AC(1:2) at different temperatures and (b) = CO Spectrum enlarged WC/AC(1:2) at different temperatures.

and WC/AC(1:2) and show some of peaks in various locations. The peaks at the 2θ of 15.1°, 15.6° and 28.7° and were corresponding to the (1 1 0), (2 1 0), (0 2 0), (2 0 0), (1 2 0), (0 2 0) and (2 1 0) faces of WO_3, the 2θ of 31.7°, 32.9°, 35.7°, 48.9°, 64.8°, 65.2°, 73.4°, 76.5° and 76.8° and are corresponding to the (0 0 1), (2 0 2), (1 0 0), (1 0 1), (1 1 0), (0 0 2), (1 1 1), (1 0 2) and (2 0 1) faces of WC.

Figure 3.4 showed the micrograph of WC/AC_x with magnification of $5.00K_x$. The FESEM further confirmed the presence of WC/AC_x and the secondary phases (W/AC_x and W_2C/AC_x) already detected by XRD. Observations of the coatings using backscattered electron (BSE) imaging allowed the identification of a matrix phase which prepared WC/AC_x from $\{W(CO)_6/AC_x\}$. This WC/AC_x phase of different composition compared to the bulk material. The bright areas belong to matrix areas with a high proportion of W (the element with the higher mean atomic number). The WC/AC_x grains were located inside the splats, where the temperature attained is insufficient to dissolve the grains. W_2C/AC_x was detected around the WC/AC_x grains [26].

FTIR of CO_2 Hydrogenation Using Prepared WC/AC: Figure 3.4 shows the spectrum obtained for the surface of the WC/AC(1:2) catalyst during the carbon dioxide hydrogenation reaction at 100°C-400°C. The carbon dioxide hydrogenation reaction is assigned to adsorbed carbon monoxide, where observed a for difference WC commercial and WC/AC(1:2) in temperatures when comparing with the band formed from the adsorption of carbon monoxide as showed Fig (3.4a). In Fig (3.4a) WC/AC(1:2) peak of CO appear very clear at temperatures from 250°C to 400°C, while in the WC commercial appeared at temperatures of 350-400°C.

After prolonged outgassing at room temperature, the spectra are significantly changed (as showed (Fig 3.4b). There were peaks constant at 100 to 250°C, while observed clear change for peak from 300 to 400 °C. According to previous studies by Shi *et al* (2010), showed adsorption of carbon monoxide (CO) when the region between 2070–2080 cm^{-1}. The study of catalysts has been completed by adsorption of CO coupled to IR spectroscopy. The spectra of surface species arising from CO adsorption over reduced catalysts are shown in (Fig 3.4b). In the region 2000–2100 cm^{-1}, a main CO band appears split at about 2050 to 2080 cm^{-1}, the first component being more intense. Bands can be assigned to CO linearly adsorbed over reduced metal center [27], [28], [29] and [30].Where the form CO appeared on two peaks are close to each other. For CO_2 and H_2 mixture, the main reaction for carbon monoxide and water formation was (as shown in equation 3.1); Reverse Water Gas Shift Reaction (RWGSR).

$$CO_2 + H_2 \rightarrow CO + H_2O. \quad (3.1)$$

Calculation of RWGS activation energy and Rate of Reaction: RWGS was the best for WC/AC(1:2) catalyst, so we used it for evaluation of RWGS activation energy at various temperatures. Table 3.2 lists the calculated RWGS reaction rate constants (k) for WC/(1:2) catalyst at various temperatures. These results indicated that by decreasing the catalyst particle size WC/AC(1:2) catalyst, RWGS reaction rate constants (k) decreased and as a result the RWGS activity of catalysts decreased. The temperature dependence of the reaction rate constants was evaluated according to the Arrhenius-type equation:

$$k = Ae^{(-Ea/RT)}; \quad (3.2)$$

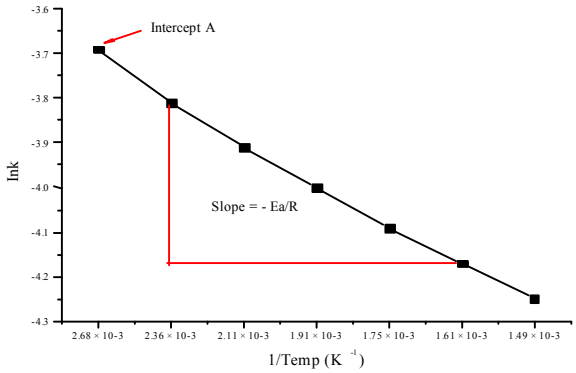

Fig. 3.5: Rate reaction analysis of RWGS activity

Table 3.2: RWGS kinetics data obtained from the RWGS model or K values calculated at different temperatures.

A	B	C	D	k	In k
100	373	2.68	40	0.025	-3.69
150	423	2.36	45	0.022	-3.81
200	473	2.11	50	0.020	-3.91
250	523	1.91	55	0.018	-4.00
300	573	1.75	60	0.017	-4.09
350	623	1.61	65	0.015	-4.17
400	673	1.49	70	0.014	-4.25

Where, A= Temperature (°C), B= Temp (K), (K = °C+273), C= 1/temp (K^{-1}) ×10^{-3}, D= Time (sec), k =1/time (sec^{-1}), In k = In (1/time).

Calculate the slope of the line produced by plotting lnk vs. 1/T and set this equal to $-E_a/R$. The activation energy was calculated to be about (-27.94 kJ/mol) for WC/AC(1:2) catalyst.

$$\text{In } k_2/k_1 = -\text{Ea}/R \times (1/T_2 - 1/T_1); \quad (3.3)$$
$$-4.17/-3.81 = -\text{Ea}/R \times (1.61 \times 10^{-3} - 2.36 \times 10^{-3})$$
$$-\text{Ea}/R = \text{Slope} = -1456.317585 \tilde{} -1459$$

$$\text{Ea} = -(\text{slope} \times 2.303R); \quad (3.4)$$
$$\text{Ea} = -(-1459 \times 2.303 \times 8.314) = 27935.6801 \text{ J mol}^{-1} = 27.935 \text{ kJmol}^{-1} \tilde{} 27.94 \text{ kJmol}^{-1}$$
$$\text{Ink} = -\text{Ea}/RT + \text{In A}. \quad (3.5)$$

$$-3.69 = [-(27935.68018)/(8.314 \times 373)] + \text{InA}$$
$$\text{In A} = -9.010210185 + 3.69 = -5.320210185$$
$$A = \hat{e}(-5.320210185) = 4.8917 \times 10^{-3} \text{ sec}^{-1}.$$

The dependence in temperatures were obtained by tracing the logarithm of k according the versus of the temperature, this layout is represented in (Fig 3.5). Thus, in order to observe the effects of temperature on the rate of reaction, a plot of reaction rate vs. temperature was constructed for this experiment (Fig 3.5).

Mechanism of CO_2 Formation in Reverse Water Gas Shift Reaction over WC Prepared Catalyst at Low Temperature Water Gas Shift Reaction: It indicates that W atoms provide active site to dissociate CO_2, while the reduction of oxidized W catalyst has to be faster than the oxidation process. Hydrogen was proposed to be only a reducing reagent without direct participation in the formation of intermediates in the RWGS reaction. The redox mechanism for the RWGS reaction has been simply modeled by following equations:

$$4\backslash 2\ CO_2 + WC \rightarrow WO_2 + 2CO \text{ OR}$$
$$3\ CO_2 + WC \rightarrow WO_3 + 6\backslash 2\ CO \quad (3.6)$$

$$2H_2 + WO_2 \rightarrow W + 2H_2O \text{ OR } 3H_2 + WO_3 \rightarrow W + 3H_2O \quad (3.7)$$

CONCLUSION

The catalytic activity of this supported catalyst was investigated via hydrogenation CO_2 reactions. It is concluded that catalysts prepared WC/AC(1:2) showed the best catalytic activity than tungsten commercial, which resulted in the production of reverse water gas shift (RWGS) reaction. RWGS rate was found to provide an improved description of the RWGS kinetic data. These results indicated that by decreasing the catalyst particle size, the activation energy of RWGS reaction increased and as a result, the reaction rate decreased consequently. The main role of K_2O is to provide active sites for formation of formates and adsorption of CO_2. Hydrogen dissociatively adsorbed on WC/AC(1:2) can be spilled over to K_2O to associate with CO_2, resulting in formation of formate species. Potassium acts as a promoter for RWGS production on WC/AC(1:2). The overall activation energy for RWGS production from CO_2 and H_2 on WC/AC-K is found to be -27.94 kJ/mol. The influence of CO on RWGS production from CO_2 + H_2 mixture on potassium-modified WC/AC(1:2).

ACKNOWLEDGMENT

The authors would like to acknowledge Ministry of Higher Education in Libya for scholarship.

REFERENCES

1. Matus, K.J.M., X. Xiao and J.B. Zimmerman, 2012. Green chemistry and green engineering in China: drivers, policies and barriers to innovation. Journal of Cleaner Production, 32(0): 193-203.

2. Cazetta, A.L., O.P. Junior, A.M. Vargas, A.P. da Silva, X. Zou, T. Asefa and V.C. Almeida, 2013. Thermal regeneration study of high surface area activated carbon obtained from coconut shell: characterization and application of response surface methodology. Journal of Analytical and Applied Pyrolysis, 101: 53-60.
3. Matos, J., C. Nahas, L. Rojas and M. Rosales, 2011. Synthesis and characterization of activated carbon from sawdust of Algarroba wood. 1. Physical activation and pyrolysis. Journal of hazardous materials, 196: 360-369.
4. Reddy, K.S.K., A. Al Shoaibi and C.A. Srinivasakannan, 2012. Comparison of microstructure and adsorption characteristics of activated carbons by CO_2 and H_3PO_4 activation from date palm pits. New Carbon Materials, 27(5): 344-351.
5. Didziulis, S.V. and K.D. Butcher, 2013. A perspective on the properties and surface reactivities of carbides and nitrides of titanium and vanadium. Coordination Chemistry Reviews, 257(1): 93-109.
6. Foo, K.Y. and B.H. Hameed, 2012. Preparation of activated carbon by microwave heating of langsat (Lansium domesticum) empty fruit bunch waste. Bioresource Technology, 116(0): 522-525.
7. Zubrin, R., B. Frankie and T. Kito, 1997. Mars In-Situ Resource Utilization Based on the Reverse Water Gas Shift: Experiments and Mission Applications. AIAA, pp: 97-2767.
8. Demirel, E. and N. Azcan, 2012. Thermodynamic Modeling of Water-Gas Shift Reaction in Supercritical Water. San Francisco, USA. Proceedings of the World Congress on Engineering and Computer Science, II: 24-26.
9. Doty, F.D., G.N. Doty, J.P. Staab and L.L. Holte, 2010. Toward Efficient Reduction of CO_2 to CO for Renewable Fuels. In ASME 2010 4th International Conference on Energy Sustainability, American Society of Mechanical Engineers, (803): 775-784.
10. Luengnaruemitchai, A., S. Osuwan and E. Gulari, 2003. Comparative studies of low-temperature water–gas shift reaction over Pt/CeO_2, Au/CeO_2 and Au/Fe_2O_3 catalysts. Catalysis Communications, 4(5): 215-221.
11. Bustamante, F., R. Enick, K. Rothenberger, B. Howard, A. Cugini, M. Ciocco and B. Morreale, 2002. Kinetic study of the reverse water gas shift reaction in high-temperature, high-pressure homogeneous systems. Fuel Chemistry Division Preprints, 47(2): 663-664.
12. Smith, R.J., M. Loganathan and M.S. Shantha, 2010. A review of the water gas shift reaction kinetics. International Journal of Chemical Reactor Engineering, 8(1): 1-34.
13. Bustamante, F., R.M. Enick, R.P. Killmeyer, B.H. Howard, K.S. Rothenberger, A.V. Cugini, B.D. Morreale and M.V. Ciocco, 2005. Uncatalyzed and wall-catalyzed forward water–gas shift reaction kinetics. AIChE Journal, 51(5): 1440-1454.
14. Tingey, G.L., 1966. Kinetics of the Water—Gas Equilibrium Reaction. I., 1966. The Reaction of Carbon Dioxide with Hydrogen. The Journal of Physical Chemistry, 70(5): 1406-1412.
15. Batista, M.S., E.M. Assaf, J.M. Assaf and E.A. Ticianelli, 2006. Double bed reactor for the simultaneous steam reforming of ethanol and water gas shift reactions. International Journal of Hydrogen Energy, 31(9): 1204-1209.
16. Sukiran, M., 2008. Pyrolysis of Empty Oil Palm Fruit Bunch using the Quartz Fluidized-fixed Bed Reactor. Master Thesis,University of Malaya.
17. Azali, A., A.B. Nasrin, Y.M. Choo, N.M. Adam and S.M. Sapuan, 2005. Development of gasification system fuelled with oil palm fibres and shells. American Journal of Applied Sciences, 72–75 (special issue).
18. Trangkaprasith, K. and O. Chavalparit, 2010. Heating Value Enhancement of Fuel Pellets from Frond of Oil Palm. In Proceedings of International Conference on Biology, Environment and Chemistry (ICBEC 2010).
19. James, A.K., R.W. Thring, P.M. Rutherford and S.S. Helle, 2013. Characterization of Biomass Bottom Ash from an Industrial Scale Fixed-Bed Boiler by Fractionation. Energy & Environment Research, 3(2): 21-32.
20. Kalanatarifard, A. and G.S. Yang, 2012. Identification of the Municipal Solid Waste Characteristics and Potential of Plastic Recovery at Bakri Landfill, Muar, Malaysia. Journal of Sustainable Development, 5(7): 11-17.
21. Swiatkowski, A., M. Pakula, S. Biniak and M. Walczyk, 2004. Influence of the surface chemistry of modified activated carbon on its electrochemical behaviour in the presence of lead (II) ions. Carbon, 42(15): 3057-3069.
22. Figueiredo, J.L., M.F.R. Pereira, M.M.A. Freitas and J.J.M. Orfao, 1999. Modification of the surface chemistry of activated carbons. Carbon, 37(9): 1379-1389.

23. Zheng, X., S. Zhang, J. Xu and K. Wei, 2002. Effect of thermal and oxidative treatments of activated carbon on its surface structure and suitability as a support for barium-promoted ruthenium in ammonia synthesis catalysts. Carbon, 40(14): 2597-2603.
24. López, F., F. Medina, M. Prodanov and C. Güell, 2003. Oxidation of activated carbon: application to vinegar decolorization. Journal of Colloid and Interface Science, 257(2): 173-178.
25. Wang, Z.M., N. Yamashita, Z.X. Wang, K. Hoshinoo and H. Kanoh, 2004. Air oxidation effects on microporosity, surface property and CH_4 adsorptivity of pitch-based activated carbon fibers. Journal of Colloid and Interface Science, 276(1): 143-150.
26. Bonache, V., M.D. Salvador, J.C. García, V. García, E. Sánchez and M. Vicent, 2010. Study of Erosion Behaviour of Conventional and Nanostructured WC-12Co Coatings Sprayed by Atmospheric Plasma. Key Engineering Materials, 423: 35-40.
27. Pászti, Z., O. Hakkel, T. Keszthelyi, A. Berkó, N. Balázs, I. Bakó and L. Guczi, 2010. Interaction of Carbon Monoxide with Au(111) Modified by Ion Bombardment: A Surface Spectroscopy Study under Elevated Pressure†. Langmuir, 26(21): 16312-16324.
28. Ozensoy, E. and E.I. Vovk, 2013. In-Situ Vibrational Spectroscopic Studies on Model Catalyst Surfaces at Elevated Pressures. Topics in Catalysis, 56(15-17): 1569-1592.
29. Eliche-Quesada, D., J. Mérida-Robles, P. Maireles-Torres, E. Rodrıguez-Castellón, G. Busca, E. Finocchio and A. Jiménez-López, 2003. Effects of preparation method and sulfur poisoning on the hydrogenation and ring opening of tetralin on NiW/zirconium-doped mesoporous silica catalysts. Journal of Catalysis, 220(2): 457-467.
30. Lai, S., S.E. Kleijn, F.T. Öztürk, V.C. Van Rees Vellinga, J. Koning, P. Rodriguez and M. Koper, 2010. Effects of electrolyte pH and composition on the ethanol electro-oxidation reaction. Catalysis Today, 154(1): 92-104.